
A numerical procedure to reduce the noise emitted by External Gear Pumps

Emma Frosina^a, Francesca Pedrielli^b, Eleonora Carletti^b, Pietro Marani^b, Luca Romagnuolo^a, Adolfo Senatore^c

^a*Department of Engineering, University of Sannio, Italy, frosina@unisannio.it*

^b*STEMS Institute - National Research Council of Italy, Ferrara, Italy*

^c*Department of Industrial Engineering, University of Naples Federico II, Italy*

Abstract

External gear pumps offer very good performance at competitive costs, making them widely spread worldwide. On the other hand, these machines are generally characterized by high levels of vibrations and noise emissions. This article presents a numerical methodology based on lumped parameter approach to optimize both spur and helical External Gear Pumps (EGPs). The methodology was implemented in a multi-environment tool called EgeMATor MP+, developed by the Fluid Power Research Group of the Universities of Naples and Sannio. This tool executes a closed-loop procedure, which starts from the pump drawing. Thanks to several subroutines developed in different interconnected environments, it permits global analysis and later optimizes EGPs.

A reference pump was optimized, acting on the geometry of the pressure relief grooves of the wear plate, with the objectives of reducing flow ripple fluctuations, pressure spikes, and crossflow. Finally, both reference and optimized pumps were tested in the CNR-STEMS research institute laboratory in Ferrara, using a specific test rig, which physically isolates the pump from the prime mover. Sound pressure levels were measured in several points surrounding each pump and the results showed an effective reduction of the emitted noise for the optimized design.

Keywords. Helical EGPs; lumped parameter numerical approach; fluid-borne noise; flow ripple reduction; design optimization.

1. INTRODUCTION

Noise emission is increasingly becoming critical in selecting components for fluid power systems. The main noise sources in these systems are generally positive displacement machines such as external gear pumps (EGPs). They are usually chosen as the hydraulic power source for fluid systems thanks to their high volumetric efficiency, durability, compactness, and low manufacturing cost. These characteristics have allowed this type of pump to be widely used in the fluid power field for both industrial and mobile applications. One of the weak points of these pumps is the relatively high sound pressure level produced

in the different working conditions in which they are used. Reducing the noise emissions without impacting the global performance of the pumps is arduous. To reach this objective, the scientific community has devised two different approaches to decrease the pressure ripple, which is considered the main noise cause. The first utilizes a three-dimensional CFD approach to evaluate the overall flow behavior and the pressurization in the variable displacement chambers. The 3D-CFD approach was used by Frosina et al. [1] to investigate the performance of a high-pressure EGP with spur gears. Heisler et al. [2] and Qi et al. [3] used different methodologies based on the same approach to predict the behavior of a helical EGP. This methodology has demonstrated to obtain an exhaustive description of those pumps, with excellent accuracy in predicting the working characteristics. These outcomes require relevant computational power and time; thus, these models usually use some kind of simplification to reduce them. The second methodology implements a lumped parameter approach, where the pressure variations within the pump are obtained from the variations of interconnected control volumes with constant properties. This methodology only necessitates a small fraction of the computational capacity required by a 3D-CFD approach, therefore permitting it to run fast simulations. A lumped parameter model that predicts the general behavior of EGP was developed and validated by Borghi et al. [4]. A similar model was developed by Battarra e Mucchi [5] that is also capable of analyzing helical gears. Ransgnola et al. [6] used a lumped parameter approach in a multi-domain system to compare helical and spur EGPs, demonstrating the flexibility and accuracy of this methodology. The authors also explored the analysis of EGPs by means of a lumped parameter approach, developing a simulation tool [7][8] called EgeMATor MP+. This tool permits fully analyzing and predicting both the fluid dynamics and mechanical behavior of EGPs with both spur and helical gears. The software allows the evaluation of gear positions by calculating the bearing's force reactions, and it also includes a procedure to optimize the pump timing given a gear tooth profile. The developed tool was used to analyze a reference helical EGP manufactured by Hydreco Hydraulics Italia. The optimization subroutine was subsequently executed, hence identifying a new design for the pressure relief grooves. The new design was prototyped, and both reference and optimized pumps were tested in the CNR-STEMS laboratories in Ferrara using a specific test rig that physically isolates the pump from the prime mover. This experimental campaign measured both flow rate and sound pressure levels (SPLs). Sound pressure levels were measured at several points surrounding each pump. The results showed good agreement with the simulation results, pointing out an effective reduction of the emitted noise for the optimized design.

2. ANALYZED PUMP

The experimental campaign proposed in this paper was performed on two different EGPs: a reference helical external gear pump designed by Hydreco Hydraulics Italia company and a prototype optimized version that differs only in the design of the pressure relief grooves. The displacement of the tested pumps is $14.5 \text{ cm}^3/\text{rev}$, with a maximum continuous pressure of 260 bar and a maximum rotational speed of 3500 rev/min. An exploded view of the reference pump is shown in Figure 2.1. Pumps have a housing made from die-cast alloy, while the front and rear covers are made of cast iron, allowing them to reach higher pressure while maintaining a relatively small total weight, making them ideal for mobile applications.

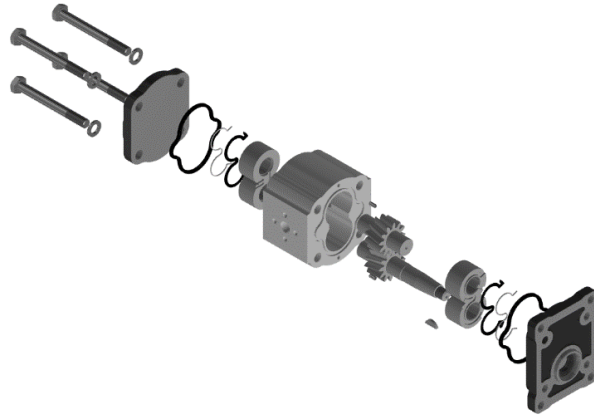


Figure 2.1. Exploded view of the reference pump

3. NUMERICAL MODEL

3.1. Overview of *EgeMATor MP+*

EgeMATor MP+ (External Gear Machine Multi Tool Simulator for Multiple Gears' Profiles) is a tool developed from scratch by the authors for the numerical simulations of external gear machines [7][8]. The tool consists of several subroutines developed in different environments, interconnected to each other, as shown by its workflow in Figure 3.1. Firstly, a subroutine called *Surface Tool*, written in the MATLAB® environment, is executed. It receives the pump geometrical data in Excel spreadsheet table format, while 2D CAD DXF files supply the tooth profile and the pressure relief grooves geometry to the subroutine. The subroutine first evaluates the meshing of the gears, checking for the presence of potential interference. After checking the gears' typology (spur or helical gear type), the *Surface Tool* calculates all the control volumes and their connections as a function of the rotation angle; then, it generates the data required. The hydraulic simulation main subroutine was developed in the simulation environment Simcenter Amesim®, based on the control volume approach. It computes the fluid-dynamic properties of the pump (pressure, flow rate, leakages, etc.) as a series of resistive and capacitive elements connected and ends up creating tables of the fluid-dynamic characteristics of the pump for post-processing and subsequent subroutines. Another subroutine was also written in the MATLAB® environment, where the forces and torques acting on the gears were evaluated. After this process, the data evaluated are passed to the "*fnest*" subroutine, which calculates the bearings reactions and thus estimates the position of the gears inside the case through an iterative finite element numerical simulation. *EgeMATor MP+* was developed to work in a closed loop; therefore, after this last subroutine, it compares the calculated gears' position with the previous step, and if the convergence is not reached, the loop procedure runs until the residuals are low enough. Further details are available in the authors' previous works [7][8].

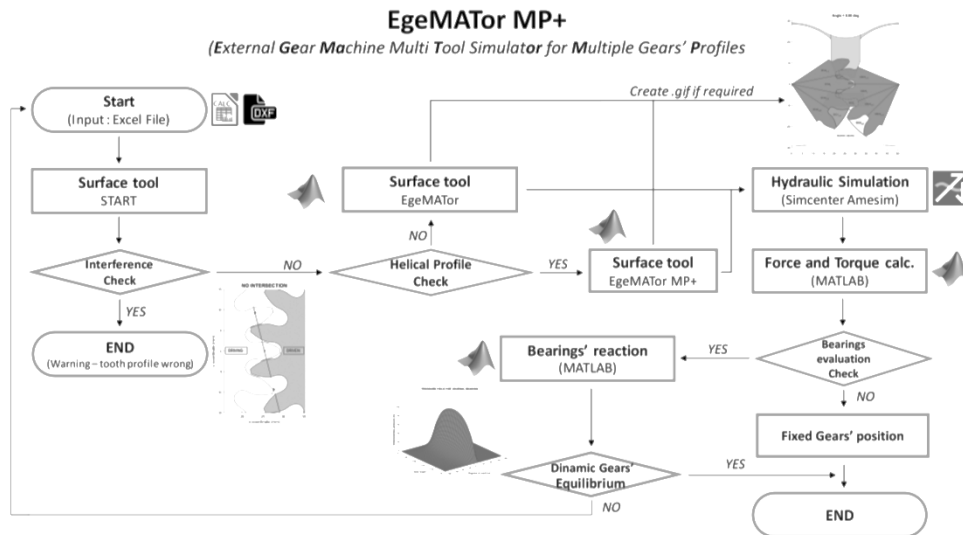


Figure 3.1. The EgeMATor MP+ (External Gear Machine Multi Tool Simulator for Multiple Gears' Profiles) workflow

3.2. *Optimal groove design research methodology*

The developed numerical model for studying and analyzing EGPs was also designed to include further capabilities, such as optimization procedures. The methodology implemented in the developed tool allows the optimization of the pressure relief grooves inside the pump wear plates for a given gear tooth profile. This procedure was based on geometric assumptions to minimize the crossflow between delivery and suction while limiting pressure spikes during the meshing of the gears. A brief description of the internal connections implemented in the lumped parameters model is required to describe the optimization methodology and its equations in more detail. Further details are available in the authors' previous works [7][8][9].

The previously mentioned *Surface Tool* estimates the volume of a displacement chamber as a function of the rotation angle φ . The optimization starts by finding the rotation angle value, which corresponds to the minimum value of the chamber volume. The identified angle, $\varphi_{DC\ MIN}$, represents the angle at which the instantaneous switch between delivery and suction pressure occurs, representing thus one of the defining parameters for a correct design of the pressure relief grooves. The optimization of the wear plate design around this angle value is of utmost importance to prevent high-pressure spikes and backflow. The next step implements the start of an iterative procedure. This procedure requires parametrizing the pressure relief grooves geometries, as shown. The relief grooves are manufactured into both wear plates, as shown in Figure 3.2. The parameterization was chosen to be normalized against the gear module m to be pump size independent and the grooves dimensions vary within the range shown in Table 3.1.

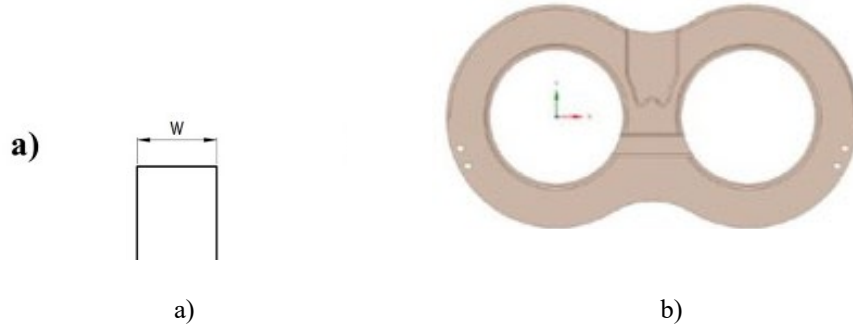


Figure 3.2. Parameters for the groove shape design search: a) Parameters for the optimization procedure; b) Wear plate design with the relief grooves

Table 3.1. Grooves parametrization

DESCRIPTION	VALUE	MIN	MAX
Delivery Groove width	W	1	3
Suction Groove height	h	0.5	2
Delivery Groove reference distance	d ₁	0	3
Suction Groove reference distance	d ₂	0	3

To optimize the groove design, a simple rectangular-shaped groove design was chosen for both the delivery and inlet groove. The range of the parameters permitted the evaluation of a large number of designs that were tested within the iterative procedure against a series of target functions:

$$TF_1 = |\varphi_{DC_MIN} - \varphi_{GRV}| \quad (3.1)$$

$$TF_2 = \frac{1}{n} \sum_{i=1}^n A(\varphi_{DC_MIN} \mp n\Delta\varphi) - A_g(\varphi_{DC_MIN} \mp n\Delta\varphi) \quad (3.2)$$

The target function TF_1 in equation (3.1) was implemented to check the volumetric efficiency of the tested design. The TF_1 needs to be as small as possible to achieve high volumetric efficiency value. This implies reducing the angular difference between the rotation angle value of minimum chamber volume φ_{DC_MIN} and the characteristics rotation angle value for the grooves φ_{GRV} , thus reducing the amount of backflow from delivery to the inlet side. In particular, for the delivery groove, φ_{GRV} represents the rotation angle of connection closure between the groove and the delivery chamber. In contrast, φ_{GRV} represents the rotation angle of connection opening between the groove and the delivery chamber for the suction groove. The target function TF_2 in equation (3.2) was implemented to minimize the internal pressure peaks occurring during gears' meshing in the proximity of φ_{DC_MIN} ; the function evaluates the cross-sectional area in dark red in Figure 3.3 (called A_g) and the projection area of the displacement chamber volumes on the lateral side in green (called A). The reduction of the pressure peaks requires this difference to be as small as possible for a number n of points with an angular pitch distance from φ_{DC_MIN} equal to $\Delta\varphi$,

with both values chosen as user input. This ensures a more gradual transition between the delivery and inlet area around the $\varphi_{DC\ MIN}$, reducing thus the pressure peaks; sign minus or plus in equation (3.2) are respectively for the delivery or suction grooves. The iterative procedure checked all the designs and then selected the one that permitted obtaining the minimum total value for the sum of both target functions. In this way, the methodology allowed identifying the optimal starting and ending positions for the pump pressure relief groove design.

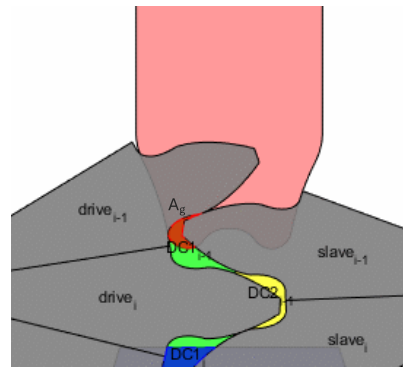


Figure 3.3. Areas evaluated in the optimal groove design methodology.

4. VALIDATION

The optimization procedure was tested on the reference pump, obtaining a new and optimized geometry. The results of this optimization procedure led to a radical change of the design philosophy: from a symmetrical design of the pressure relief grooves geometries, for the reference pump, to an asymmetrical one on which the front and rear wear plates exhibit pressure relief grooves with noteworthy geometric differences between them, as shown in Figure 4.1. The validation of the optimization methodology was carried out in two phases: in the first phase, the new design was compared to the reference pump through numerical models; in the second phase, an experimental campaign was performed, allowing to test and acquire the flow rate and the noise emissions of the tested pumps.

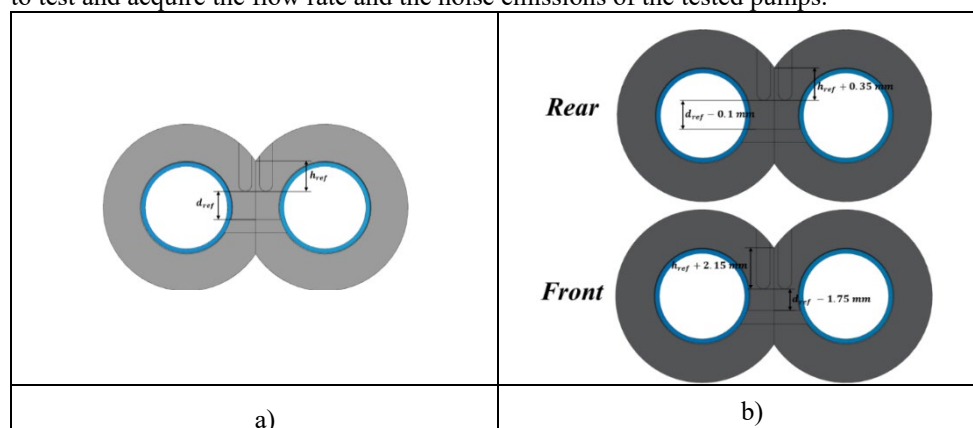


Figure 4.1. Relief grooves design: reference pump (left) and optimized design (right).

4.1. Numerical model validation

The first phase was carried out by simulating several working conditions; the results of the two designs were compared. To focus on the primary aspects investigated by the optimization methodology, the comparison examined the mean flow rate value, the non-uniformity of the flow rate, and the pressure evolution inside the variable displacement chamber. This work shows only the comparison results obtained for a pump speed of 1500 rev/min and a system delivery pressure of 200 bar since the main target of the present work was the optimization of the design in this operating condition that was critical for the pump. However, the same analysis has been performed for different pressures and rotational speeds. The flow rate is normalized to a reference value, Q_{ref} , for confidential reasons. Figure 4.2 shows the numerical comparison between the reference and optimized design of the flow ripple for a particular operating condition.

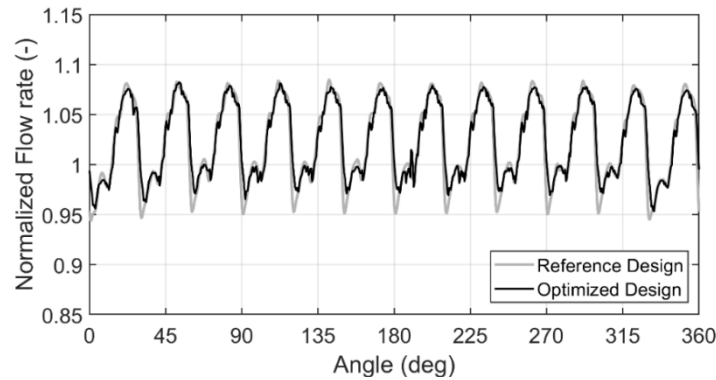


Figure 4.2. Numerical flow ripple comparison at $n=1500$ rev/min, $\Delta p=200$ barA

The comparison shows that the optimized design exhibits improved performances for both analyzed physical dimensions, with an increase of about 0.5% of the mean delivery flow rate and a reduction of the non-uniformity of the flow ripple of around 8%. In particular, the non-uniform rate reduction was mainly due to a higher minimum value of the flow ripples. This aspect implies a lower backflow rate value, one of the aspects on which the optimization methodology was focused.

Figure 4.3 presents another significant result: the comparison of the numerical pressure evolution inside the variable displacement chamber around the meshing zone between the reference and optimized pumps; in particular, on the left, there are results for the driving while on the right for the driven gear. The comparison highlights a reduction of the pressure spikes during the meshing of both gears, further suggesting the validity of the methodology employed. The reduction was mainly relevant for the driving gear chamber, with a reduction of about 10% of the pressure spikes. This result, coupled with the decrease in the non-uniformity rate of the flow ripple, hinted at the possibility of lower vibrations for the optimized design and, hence, a reduction in noise emissions.

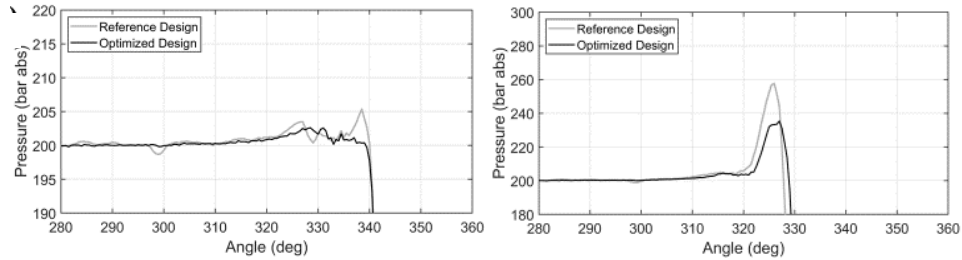


Figure 4.3. Numerical pressure evolutions comparison at $n=1500$ rev/min, $\Delta p=200$ barA: Driving gear (left); driven gear (right).

4.2. Experimental validation

This section focuses on the comparison between the noise emitted by a reference pump and an optimized one.

4.2.1. Test rig and experimental design

The experimental campaign to validate the model was performed on a dedicated test rig in the CNR-STEMS laboratories. This test rig was built for testing gear pumps, which are mounted on a metal plate and placed inside a large shed. It was explicitly designed to acoustically isolate the pump under test from the prime mover and all other hydraulic components placed outside the shed and separated by a concrete wall. This layout exclusively permits the acquisition of the noise radiated from the pump. The flow rate was acquired thanks to a screw-type flow meter installed on the pressure line; the circuit also integrates pressure and temperature transducers. The tests were conducted with an oil temperature of $40\text{ }^{\circ}\text{C} \pm 3\text{ }^{\circ}\text{C}$, thanks to an off-line cooling system. The environmental conditions were almost constant throughout the test, with air temperature ranging from $4\text{ }^{\circ}\text{C}$ to $9\text{ }^{\circ}\text{C}$ and relative humidity values ranging from 80 % to 94 %. The hydraulic scheme of the test rig is reported in Figure 4.4.

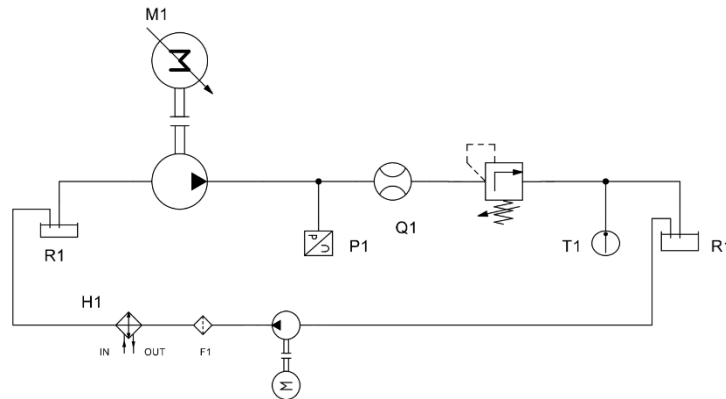


Figure 4.4. Test bench layout

For each pump type (reference and prototype), the tests were repeated on two different units to have a more reliable characterization and to compensate for possible production errors.

Noise tests were performed in 36 different operating conditions: six different rotational pump speeds (500, 1000, 1500, 1800, 2000, and 2200 rev/min) and, for each speed, six different delivery pressures (10, 50, 100, 150, 200, and 240 bar), from no-load condition to maximum continuous pressure. For each pump type and unit and each operating condition, the acquisition was repeated twice, the first run with an ascending delivery pressure and the second with a descending delivery pressure at fixed rotational speed.

4.2.2. Noise measurements

The noise tests consisted of the simultaneous acquisition of the SPL in five different positions arranged at a distance of 30 cm from the noise source in every direction (front, right, left, top, bottom) in order to account for the directivity of the noise emissions for each pump. Figure 4.5 shows the measurement layout.

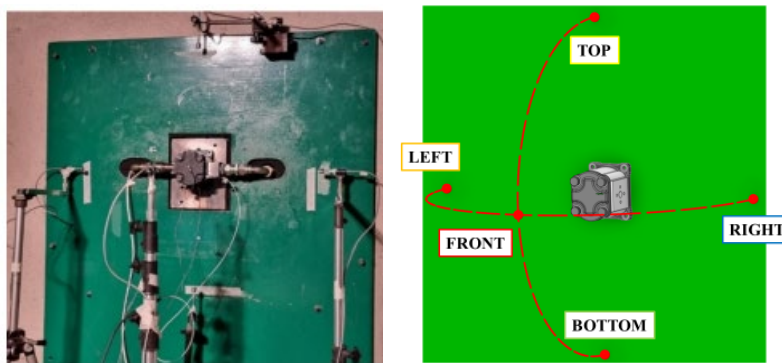


Figure 4.5. Noise measurement acquisition layout

The evaluation of the differences in noise emission between the reference pump and the optimized one (prototype) was based on a series of measurements of SPLs. 720 SPL spectra were acquired for each pump type: 2 units, 36 operating conditions, two runs and five measurement positions.

At each measurement point, the background noise was stationary, with SPLs always more than 15 dB lower than the corresponding SPLs of the noise sources under test.

The instrumentation included an 8-channel Siemens SCADAS analyzer (SCM-VM8.E module) coupled with Simcenter LMS TestLab software. The free-field $\frac{1}{2}$ inch microphones (Brüel&Kjær 4181) and the measurement instrumentation met the requirements of class 1 instruments. Sound pressure measurements were performed in the frequency range of 20÷10000 Hz, and all the measurement chains were recalibrated several times during the tests with a pistonphone (Brüel&Kjær 4220). However, for this investigation, only the results in terms of linear overall SPL will be considered.

4.2.3. Measurement uncertainty

The uncertainties of sound pressure levels, in decibels, are estimated by the total standard deviation, σ_{tot} , in decibels, which should be obtained using the modeling approach described in ISO/IEC Guide 98-3 [10], which requires a mathematical model that can be replaced by results from measurements in case of lack of knowledge.

In this context, the total standard deviation is expressed by the standard deviation of reproducibility of the method, s_{R0} , in decibels, and the standard deviation due to the noise emission instability of the source, s_{ome} , in decibels, describing the uncertainty due to the instability of the operating and mounting conditions of the source under test, by equation (4.1).

$$s_{TOT} = \sqrt{s_{R0}^2 + s_{omc}^2} \quad (4.1)$$

The standard deviation values for s_{R0} and s_{omc} were estimated following the suggestions of the ISO Standard 3746:2010 [11]. The standard deviation s_{R0} was calculated using the existing knowledge on the noise emission of this family of machines (paragraph 9.3.2 of the Standard). In this regard, CNR-STEMS has been using this measurement method on external gear pumps for 20 years [12][13][14], and over time, researchers have had the opportunity to use the same method with different instrumentation and different operators. For this reason, a reasonable estimate of s_{R0} is 1 dB. The standard deviation s_{ome} was estimated considering a slight variation with time and properly defined measurement procedure (Note in paragraph 9.2 of the Standard). For this reason, a reasonable estimate of s_{ome} is 0.5 dB.

This leads to a total standard deviation value $s_{tot} = 1.12$ dB.

4.2.4. Noise measurement results

The first results, showing that the helical pump is quieter than the spur pump, were presented in Mazzei et al. [15]. In the following section, a comparison between the reference pump and its optimized prototype is given for each operating condition.

To evaluate the noise emission of the different pump types, an average sound pressure level SPL_{av} was taken between the two units, the two runs and the five measurement points.

Figure 4.6 shows the difference between the average SPL of the reference pump (SPL_{av-REF}) and the optimized pump ($SPL_{av-PROTO}$) for each operating condition. Positive differences indicate that the reference pump is noisier than the optimized one; negative differences show the opposite.

The shaded area indicates the uncertainty interval associated with these differences (± 1.58 dB), which is calculated following the propagation of the errors, with equation (4.2), assuming to have independent variables and assuming that the uncertainty of each quantity is quantified in terms of the total standard deviation value s_{tot} . For the results inside the shaded area, no indications can be deduced.

$$\delta SPL_{diff} = \sqrt{\delta SPL_{REF}^2 + \delta SPL_{PROTO}^2} \quad (4.2)$$

The graph in Figure 4.6 shows that the improvements occur from 1500 rev/min upwards, while below this rotational speed the differences are within the measurement uncertainty. In particular:

- Both at 1500 and 1800 rpm, the PROTO pump is less noisy than the REF pump at medium-high pressures. For 1500 rpm, the differences range between 2 and 3 dB (2.6 dB at 150 bar, 3.1 at 200 bar, and 2.5 dB at 240 bar), while for 1800 rpm, the differences are even higher (5.4 dB at 150 bar, 5.0 at 200 bar and 3.8 dB at 240

bar). The operating point on which the optimization was based (1500 rpm and 200 bar) presents good results.

- At 2000 rpm, the trend changes, and the differences are similar to those at 1500 rpm, in the range of 2-3 dB.
- At the maximum rotation speed (2200 rpm), the improvement appears increasingly apparent, especially at high pressures with differences of SPL up to almost 11 dB (6.7 dB at 150 bar, 9.2 dB at 200 bar, and 10.7 dB at 240 bar).

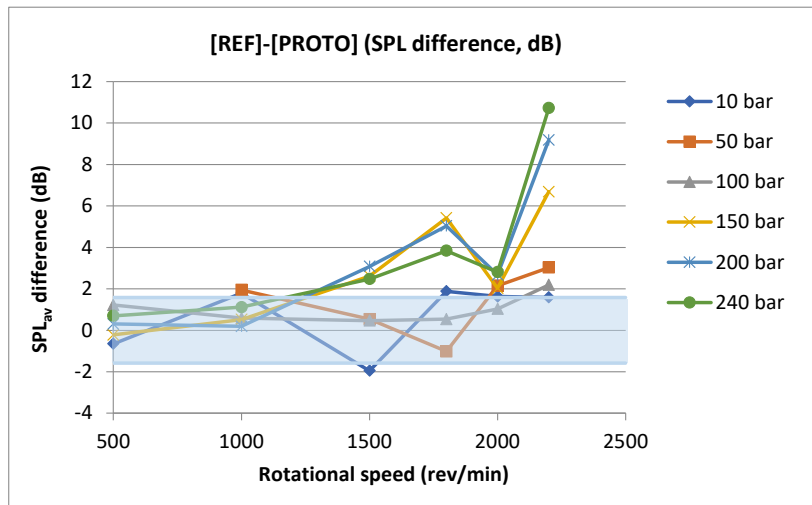


Figure 4.6. SPL_{av} difference between reference and optimized pumps for all the operating conditions

5. CONCLUSIONS

In this article, a novel numerical methodology for optimizing the noise and vibration emission of both spur and helical gear pumps was described. This methodology is based on lumped parameters approach and was implemented in a multi-environmental tool called EgeMATor MP+. This tool was developed entirely and validated by the authors; it consisted of tightly interconnected subroutines that worked in a closed-loop procedure.

The optimization subroutine was based on optimizing the design of the pressure relief grooves on the wear plates with the objective of finding the optimal design that reduces the pressure spikes, the flow ripple fluctuations, and the backflow during the meshing of the gears. The proposed methodology was employed to study and then optimize a reference helical gear pump. The optimization procedure determined a new asymmetric design that was first analyzed through the numerical tool, showing promising performances regarding noise and vibration emission reduction. The tool has been completely developed by the authors and demonstrated to be valid for optimizing EGPs. After prototyping the optimized design, an experimental campaign was organized in collaboration with the CNR-STEMS using a test rig physically isolating the tested pump from the prime mover. The results show that the proposed optimized pump has lower SPLs at 1500, 1800, and 2200 rpm with a

maximum reduction of almost 11 dB at higher rotational pump speed and pressure. This validates the methodology proposed. However, due to the complexity of the subject, specific tests and combined noise-vibration frequency analyses would be necessary to understand the reasons why, in certain conditions, there is a higher noise emission.

This will be investigated in a different specific study. Future work will also focus on further improving the optimization feature, implementing more complex pressure relief grooves designs and parametrization and target functions.

6. NOMENCLATURE

ACRONYM	DESCRIPTION
EGP	External Gear Pump
CFD	Computational Fluid Dynamic
EGM	External Gear Machine
SPL	Sound Pressure Level
SPL_{av}	Average sound pressure level

SYMBOL	DESCRIPTION	UNIT
A	Area of displacement chamber	[m ²]
A_g	Cross-sectional area of groove	[m ²]
B	Axial length of the gears	[m]
d_1	Delivery Groove reference distance	[-]
d_2	Suction Groove reference distance	[-]
h	Suction Groove height	[-]
m	Gear module	[m]
P	Pressure	[Pa]
p'	Non-dimensional pressure	[-]
Q_{ref}	Reference flow rate	[L/min]
s_{omc}	Standard deviation due to the noise emission instability of the source	
s_{R0}	Standard deviation of reproducibility	
s_{tot}	Total standard deviation	
W	Delivery Groove width	[-]
Z	Axial extension of the slices	[m]
z_1	Axial start position for the reference profile	[m]
z_2	Axial finish position for the reference profile	[m]

GREEK LETTER	DESCRIPTION	UNIT
B	Total helix rotation angle	[rad]
φ	Gear profile rotation angle	[rad]
φ_1	Axial profile angle start position for the reference profile	[rad]
φ_2	Axial profile angle finish position for the reference profile	[rad]
$\varphi_{DC MIN}$	Gear profile rotation angle of instantaneous commutation (minimum chamber volume)	[rad]
φ_{GRV}	Groove rotation angle characteristics	[rad]
$\Delta\varphi$	Angular pitch value for optimization function	[rad]

ACKNOWLEDGMENTS

The authors gratefully acknowledge the invaluable support provided by Diplomatic MS, in particular, to Simone Bulleri. The authors thanks also Pietro Mazzei.

7. REFERENCES

- [1] E. Frosina, A. Senatore, M. Rigosi, "Study of a High-Pressure External Gear Pump with a Computational Fluid Dynamic Modeling Approach", *Energies*, 2017, 10(8), 1113. 10.3390/en10081113
- [2] A.S. Heisler, J.J. Moskwa, F.J. Fronczak, "Simulated Helical Gear Pump Analysis Using a New CFD Approach", ASME 2009 Fluids Engineering Division Summer Meeting. Volume 1: Symposia, Parts A, B and C. Vail, Colorado, USA. August 2–6, 2009. pp. 445-455. 10.1115/FEDSM2009-78472
- [3] F. Qi, S. Dhar, V. Nichani, C. Srinivasan, W. De Ming, L. Yang, B. Zhonghui, J.Y. Jinming, "A CFD study of an Electronic Hydraulic Power Steering Helical External Gear Pump: Model Development, Validation and Application", *SAE Int. J. Passeng. Cars - Mech. Syst.* 9(1):346-352, 2016, 10.4271/2016-01-1376.
- [4] M. Borghi, B. Zardin, E. Specchia, "External Gear Pump Volumetric Efficiency: Numerical and Experimental Analysis", *SAE Technical Papers*, 2009. 10.4271/2009-01-2844.
- [5] M. Battarra, E. Mucchi, "A method for variable pressure load estimation in spur and helical gear pumps", *Mechanical Systems and Signal Processing*, Volumes 76–77, 2016, Pages 265-282, ISSN 0888-3270, 10.1016/j.ymsp.2016.02.020.
- [6] T. Ransegnola, X. Zhao, A. Vacca, "A comparison of helical and spur external gear machines for fluid power applications: Design and optimization", *Mechanism and Machine Theory*, Vol.142, 2019, 103604, ISSN 0094-114X, 10.1016/j.mechmachtheory.2019.103604.
- [7] G. Marinaro, E. Frosina, A. Senatore, "A Numerical Analysis of an Innovative Flow Ripple Reduction Method for External Gear Pumps", *Energies*, 2021, 14, 471. 10.3390/en14020471.
- [8] P. Mazzei, E. Frosina, S. Bulleri, A. Senatore, "Numerical Modeling of Helical External Gear Pump Through a Lumped Parameter Approach", 2022 IEEE GFPS Symposium, Naples, Italy 12-14 October 2022.
- [9] P. Mazzei, E. Frosina, A. Senatore, 2023, Helical Gear Pump: A Comparison between a Lumped Parameter and a Computational Fluid Dynamics-Based Approaches, *Fluids MPDI*, 8(7).
- [10] ISO/IEC Guide 98-3:2008, Uncertainty of measurement - Part 3: Guide to the expression of uncertainty in measurement (GUM:1995)
- [11] ISO 3746:2010, Acoustics - Determination of sound power levels and sound energy levels of noise sources using sound pressure - Survey method using an enveloping measurement surface over a reflecting plane
- [12] F. Pedrielli, E. Carletti, "Acoustical evaluation of power skiving gears for hydraulic pumps", 21st International Congress on Sound and Vibration, Beijing, China (13-17 July 2014), Session SS21, pp.1-8, ISBN 978-83-62652-66-2.
- [13] F. Pedrielli, E. Carletti, G. Brambilla, "ISO 9614-2 applied to an external gear pump: determination of type A uncertainty", 26th International Congress on Sound and Vibration ICSV26, Montreal, Canada (7-11 July 2019), pp. 1-8, ISBN 978-1-9991810-0-0, ISSN 2329-3675
- [14] F. Pedrielli, E. Carletti, G. Brambilla, "ISO 9614-2 applied to an external gear pump: effect of geometric measurement parameters on the uncertainty", 28th International Congress on Sound and Vibration ICSV28, Singapore (24-28 July 2022), pp. 1-8, ISBN 978-981-18-5070-7, ISSN 2329-3675

- [15] P. Mazzei, E. Carletti, F. Pedrielli, E. Frosina, P. Marani, A. Senatore, “Acoustical characterization of external gear pumps: comparison of spur and helical gears”, 29th International Congress on Sound and Vibration ICSV29, Praha (9-13 July 2023), pp. 1-8, ISBN 978-80-11-03423-8, ISSN 2329-3675